frontiers | Frontiers in Marine Science

TYPE Original Research
PUBLISHED 13 March 2025
DOI 10.3389/fmars.2025.1528106

OPEN ACCESS

EDITED BY
Beata Szymczycha,
Polish Academy of Sciences, Poland

REVIEWED BY
Bo-Shian Wang,
National Academy of Marine Research (NAMR), Taiwan
Li Jian,
Hainan Medical University, China

*CORRESPONDENCE
Jing-Chun Feng
fengjc@gdut.edu.cn

RECEIVED 14 November 2024
ACCEPTED 24 February 2025
PUBLISHED 13 March 2025

CITATION
Cai C, Feng J-C, Wu G, Hou R, Chen X, Liu J, Zhang X and Zhang S (2025) Combined uranium-series and trace elements analysis in cold seep bivalves: possibility in hundred-year-scale reconstruction of deep-sea temperature and acidification.
Front. Mar. Sci. 12:1528106.
doi: 10.3389/fmars.2025.1528106

Combined uranium-series and trace elements analysis in cold seep bivalves: possibility in hundred-year-scale reconstruction of deep-sea temperature and acidification

Chaofeng Cai[1], Jing-Chun Feng[1,2]*, Guozhong Wu[1], Rui Hou[1], Xiao Chen[2], Jinyi Liu[1], Xiaochun Zhang[1] and Si Zhang[2,3]

[1]School of Ecology, Environment and Resources, Guangdong University of Technology, Guangzhou, China, [2]Southern Marine Science and Engineering Guangdong Laboratory (Guangzhou), Guangzhou, China, [3]South China Sea Institute of Oceanology, Chinese Academy of Sciences, Guangzhou, China

Despite the pivotal role of deep-sea in the global climate system, effective technology is still limited for reconstructing the key parameters of deep-sea environment such as temperature and acidification, especially at the hundred-year scale. In this study, we assessed the robustness and reliability of using bivalve shells in reconstructing cold seep environments. A significant heterogeneous distribution of trace elements was observed in the shells of clams and mussels from Formosa and Haima cold seeps even if they were collected from the same site, which was caused mainly by the environmental variables rather than physiological characters. The results of the principal component analysis revealed different trace elements ratios in the shell were associated with seepage. In particular, Sr/Ca was identified as a reliable proxy for temperature reconstruction, which performed better than oxygen isotopes. Na/Ca and U/Ca are potential proxies for cold seep acidification, but further validation is needed before their practical application. The age bias using the U-series dating method resulted from high ^{232}Th and low initial ^{230}Th/^{232}Th rather than from alpha-recoil processes. The median ages assigned to mussels from the F and Haima cold seeps were 229.5 and 323.5 years, respectively. The lifespan of clams from the Haima cold seep was too short to date accurately. We proposed to conduct feasibility verification and error correction to enhance the method performance in reconstructing the hundred-year evolution of cold seep environment in the South China Sea.

KEYWORDS

deep-sea bivalves, trace elements, u-series dating, oxygen isotope, temperature reconstruction

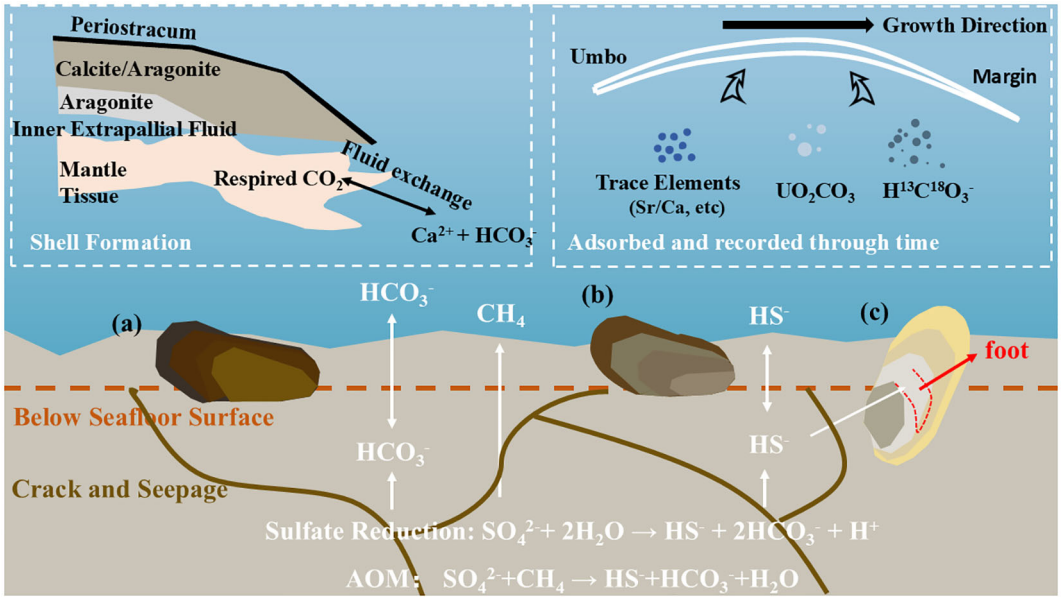

GRAPHICAL ABSTRACT
(a) mussels *Gigantidas platifrons* collected from the Formosa site **(b)** mussels *Gigantidas haimaensis* collected from Haima site are benthic species while **(c)** clams *Archivesica marissinica* collected from Haima site is burrowing species.

1 Introduction

The deep-sea, as an important part of the global climate system, profoundly impacts on ocean cycling, carbon storage, and climate regulation (Wang et al., 2021; Chen et al., 2023; Lu et al., 2023; Mashayek et al., 2024). By 2020, global temperature has already been 1.7 ± 0.1°C higher than preindustrial levels, which is anticipated to reach 2°C by the end of 2020s (McCulloch et al., 2024). As a result, the heat content inevitably increases in the polar zone and deep sea, which in turn causes a rise in the local sea level (Biló et al., 2024). However, research on deep-sea warming is still limited because current observation data from satellites or high-frequency radar are concentrated mainly in shallow sea areas. Even on the continental shelf, it is difficult to observe the temperature data via satellites or high-frequency radar, especially in the deep sea under several thousand meters. Moreover, it is challenging to conduct long-term continuous observations via current instruments due to the complex environment such as high pressure, low temperature, and seawater corrosion. To date, technologies for reconstructing the continuous long-term evolution of deep-sea temperatures are highly needed.

The foraminifera shell in the sediment has been used to reconstruct paleotemperature via isotope analysis and trace element analysis (Groeneveld et al., 2019). Using this method, the deep-sea temperatures could be measured for the first time over the past 1, 200 years (Lu et al., 2023). Foraminifera can only be used to trace environmental changes over thousands or millions of years, left powerless in studying detailed change over hundreds of years. This is attributed to slow sedimentation as the foraminifera obtained at different depths can be thousands of years apart. For example, the depth intervals of less than 50 cm in a sediment core in an Arctic cold seep represents nearly 2000 years apart (Yao et al., 2020). In addition, foraminifera obtained at different depths cannot serve as a continuous monitoring technique for non-continuous sampling in sediment. In contrast, bivalve shells can serve as a reconstruction technique to overcome these shortcomings. Previous studies have used elements/Ca (M/Ca) ratios in bivalves shell to reconstruct paleotemperature in the form of high-resolution archives to monitor the yearly, monthly and even daily changes of temperature (Lorens and Bender, 1980; Hart and Blusztajn, 1998; Marriott et al., 2004; Füllenbach et al., 2015), dissolved particles concentration (Jeffree et al., 1995; Poulain et al., 2015) and productivity (Markulin et al., 2019). In deep-sea cold seep ecosystems with abundant leakage of methane and fluids rich in reduced materials, bivalves are the most dominant and most numerous species (Boetius and Wenzhöfer, 2013; Ceramicola et al., 2018; Xu et al., 2020). Cold-seep bivalves host sulfide-oxidizing bacteria and methane-oxidizing bacteria, obtaining reduced chemicals and offering energy as well as nutrients to their host through methane or sulfide oxidation (Halary et al., 2008). Previous studies have demonstrated that cold seep bivalves can serve as potential archives of temperature in the deep sea but they have not proposed any robust reconstruction proposal (Scholz et al., 2010; Hu et al., 2015). Alternatively, it is also possible to use the trace elements to reconstruct temperatures because the availability of multiple trace elements can produce significant biological feedback (Mukherjee and Large, 2020). Moreover, the trace elements in the shell is correlated with that in the water, reflecting participation in biogeochemical cycles (Ren et al., 2024). Besides temperature, acidification can also be recorded in bivalve shell. Na/Ca and U/Ca can be used as proxies for pH and thus acidification [8, 9]. The proxy potential is further enhanced by their greater capacity to acclimate or adapt to ocean acidification through beneficial transgenerational acclimation (Zhao

et al., 2017b; Markulin et al., 2019). What's more, Na/Ca proxy is only applicable to species that can tolerate low pH, as they possess efficient H/Na exchangers in their mantles. In contrast, other species either perish or experience significantly slowed growth when pH falls below certain critical levels. A series of various environmental factors on Na/Ca is observed (temperature and food supply) (Markulin et al., 2019). Similarly, the result of U/Ca reveals species-specific differences. For example, U/Ca ratios in two *S. giganteus* shells are not under environmental control but unknown one (Gillikin and Dehairs, 2013). In general, there are limited studies on uranium in bivalve shells (especially high-resolution profile of U/Ca). It's reported that U/Ca in bivalve shells can be related to strong diagenetic trends (Labonne and Hillaire–Marcel, 2000), granite weathering and industrial effluents (Price and Pearce, 1997) and uranium pollution (Markich et al., 2002). Thus, a high resolution profile of Na/Ca and U/Ca in shells of cold seep bivalves is needed to evaluate if Na/Ca and U/Ca is related to pH in these specific species.

Before deep-sea environment reconstruction, several issues should be considered. First, the subject factors influencing the adsorption of trace elements in deep sea bivalves may differ from those in freshwater counterparts. For example, temperature or salinity is usually the dominant factor influencing freshwater bivalves, whereas food availability is the most important factor in the deep-sea environment (Gilkinson, 1986). Second, for some species, trace elements can be controlled by physiological processes rather than environmental factors, which may significantly decrease or increase with time and even become lower than the limit of detection patterns (Takesue et al., 2008; Marali et al., 2017; Barrat et al., 2023). Third, although radiocarbon technology is often applied in carbonate shell dating, this technique leads to bias in cold-seep environments. Because the seepage fluid contains dead-carbon methane from deeper sediments and is assimilated by bivalves through symbionts, the level of bias is unclear and dependent on the seepage intensity and degree of digestion.

Uranium-thorium (Th) dating is a more precise technique than radiocarbon analysis for dating range and potential dead-carbon mixed into samples (Wendt et al., 2021). The lifespan of deep-sea clam was successfully determined by δ^{228}Ra chronology (an important isotope in the U-Th decay series.), with a length of 8.4 mm reaching approximately 100 years) (Turekian et al., 1975). Cold-seep environments with relatively low oxygen levels and temperatures can nurture long-lived bivalves (Philipp and Abele, 2010). Thus they are likely to reach hundreds of years in lifespan, similar to the deep-sea clam in the reference. In U-Th dating method, whether the samples stay as a closed-system is crucial because in an open-system, the isotopes in samples can exchange with that in environment, modifying the isotopes signature. Whether mollusk carbonates stay as a closed system remains questionable. For an open system, samples can be dated well by applying an isochron or alpha-recoil redistribution model based on the data trends in the evolution diagram. A strict reference δ^{234}U value opposite to diagenesis should also be applied to omit outlier values that can result in age estimation errors (Dutton, 2015). Besides, the data can be calibrated by applying the initial ^{230}Th/^{232}Th ratio, which tends to remain constant over the hundred years of a bivalve's lifespan. However, deep-sea samples have the potential to contain higher ^{232}Th levels than surface samples do, and older deep-sea samples have more considerable age uncertainties (± several hundreds of years for samples with a few thousand ppt ^{232}Th) (Cheng et al., 2000). Therefore, the feasibility of applying U dating to cold-seep bivalves remains unclear.

In this study, a comprehensive survey was conducted to characterize the chemical properties of the shells of deep-sea bivalves captured in the South China Sea (SCS). Laser ablation-inductively coupled plasma mass spectrometry (LA-ICP-MS) was used in the trace element analysis to explore the profiles and possible subject factor for different trace elements ratios. U-Th dating was conducted to examine the feasibility of applying this technique in cold-seep bivalves. The specific aims of this study were to: (i) discuss the potential sources and subject processes affecting trace elements concentration in cold-seep bivalves; (ii) provide a reference age using the U-Th dating approach to assign the median ages of cold-seep bivalves and identify the possible sources of error; and (iii) study the potential of reconstructing the paleotemperature and acidification based on trace elements.

2 Materials and methods

2.1 Sample acquisition and pretreatment

The cold-seep bivalves were captured alive using the remotely operated grab with television and subsequently frozen and saved at -80°C and transported to the laboratory. All samples were collected in June (Formosa site) and July 2022 (Haima) on the scientific research vessel (R/V) KEXUE (Institute of Oceanology, Chinese Academy of Sciences, China). Mussels (*Gigantidas platifrons*) were collected from the F site, whereas the mussels (*Gigantidas haimaensis*) from HM-Seep site and clams (*Archivesica marissinica*) from HM-Baiguabei site, respectively. The geological setting is shown in Figure 1. In the laboratory, soft-tissues were removed from the live-collected specimens. Shells were rinsed with deionized water and air-dried. One valve of each sample, for oxygen isotope analysis, trace elements analysis and growth increments analysis, was wrapped in epoxy resin and cut along the growth axis of the ventral side using a precision cutting machine (ISOMET5000, Buehler, America) equipped with a diamond-coated wafer-thin blade. Using this method, each shell was cut into slabs. The shell slabs were ground on glass plates using suspensions of 600 and 1200-grit SiC powder and subsequently polished with Al2O3 powder (grain size of 0.05 μm) on a grinding and polishing machine (Ecome1300 Metaserv250, Buehler, America). For another valve, the margins and umbones were cut off with a hand-held cutting machine for further U-Th dating analysis. *In-situ* element analysis via laser ablation (LA)-ICP-MS.

As shown in Figure 1d, the primary and trace element compositions of clam shell slabs were measured from the umbo part (the oldest) to the margin part (the youngest) (Fritz, 2001). The trace-element line scanning of the samples was conducted via an NWR 193-nm ArF Excimer laser-ablation system coupled to an

iCAP RQ LA-ICP-MS instrument at Guangzhou Tuoyan Analytical Technology Co., Ltd. (Guangzhou, China). The LA-ICP-MS instrument was tuned using NIST 610 and NIST 612 standard glass (Jochum et al., 2011) to yield low oxide production rates. Helium carrier gas was fed into the cup at a flow rate of 0.7 L/min; subsequently, the aerosol was mixed with argon make-up gas at a flow rate of 0.79 L/min. During sampling, 14 isotopes including ^{7}Li, ^{23}Na, ^{24}Mg, ^{43}Ca, ^{55}Mn, ^{57}Fe, ^{65}Cu, ^{66}Zn, ^{88}Sr, ^{97}Mo, ^{137}Ba, ^{185}Re, ^{232}Th and ^{238}U were measured. The dwell time for each isotope was 10 ms. The laser fluency was 3 J/cm^2, with a repetition rate of 6 Hz and a 50-μm spot size corresponding to a scan speed of 10 μm/s. The raw isotope data were reduced via the "baseline subtract" and "trace elements" data reduction scheme (DRS). The DRS runs within the IOLITE package of Paton et al. (2011). In IOLITE, user-defined time intervals are established for the baseline correction procedure to calculate the session-wide baseline-corrected values for each isotope. The trace elements were calibrated with the NIST 610 as an external standard. The samples were scanned at 50 μm/s to eliminate potential contamination. To decrease the higher scatter (lower signal-to-noise ratio) of line scanning than of spot analysis, the data were smoothed via a 31-pt weighted moving average filter (Schöne et al., 2022). Values exceeding five σ values of the 31-pt running averages were regarded as outliers and this applied to less than 1% of all values. The relative standard deviations (RSD) from standard materials of NIST 610 and NIST 612 are shown in Table 1. Most samples had RSD of less than 1% except Fe ratios from 2022MH-2, which were therefore excluded from further analysis. Following this method, geometry-related sampling errors that could bias paleoenvironmental interpretations were minimized (Schöne et al., 2022). To avoid errors resulting from contamination, the points lying close to the epoxy (i.e., the first and a small number of final points) were removed. After the above processing, the data still reveal extremely high peaks at a few points. This may have something to do with the life longevity and thus contain condensed information. Therefore, the data were further smoothed via additional LOWESS processing with a window ratio of 0.05.

2.2 U-Th dating

The samples were grinded and passed through a 200-mesh sieve, and approximately 0.1 g was taken for analysis. The analytical protocol has been described in detail by Luo and Ku (1991). Powder samples were successively treated with 2 N HNO_3 leaching and HF-HNO_3-$HClO_4$ fuming to affect total dissolution. Approximately 20 mg of Fe^{3+} was added as a carrier, along with yield tracers ^{236}U and ^{229}Th. Separation and purification of U and Th were performed according to the anion exchange (Dowex AG1 x 8) procedures (Shangde et al., 1987). A solution of 8 N NHNO:-0.1N HNO, was used to separate Fe from U on the anion column. The samples were tested with a Thermo-Finnigan Neptune (Thermo Fisher Scientific, America). Standard samples of U-metal SRM-960, YB-1, and HU-1 were used to monitor the precision of the instrument. Values exceeding five σ values of the 31-pt running averages were regarded as outliers and this applied to less than 1% of all values. The relative standard deviations (RSD) from standard materials of NIST 610 and NIST 612 are shown in Table 1. Most samples had RSD of less than 1% except Fe ratios from 2022MH-2, which were

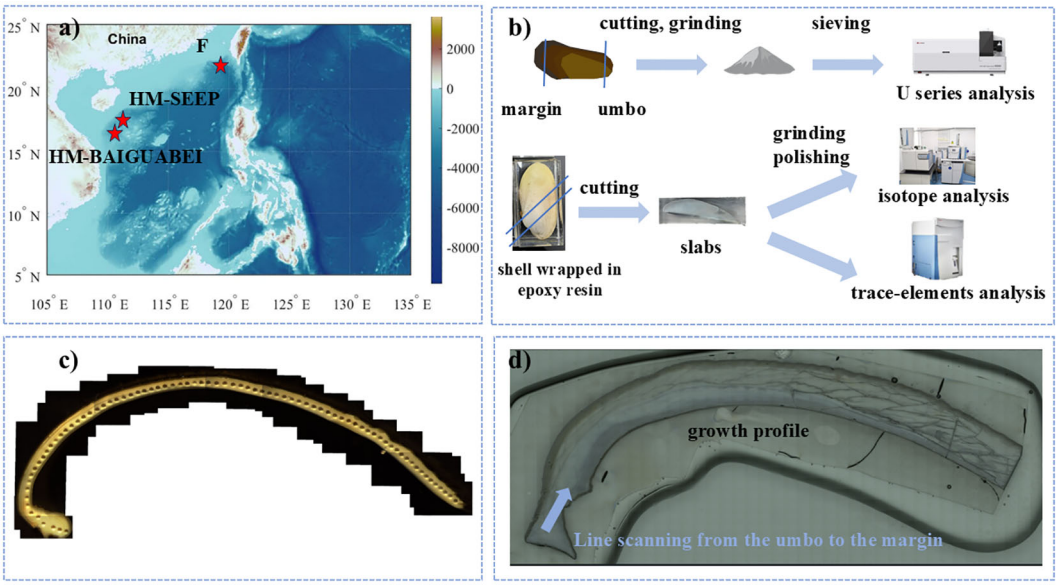

FIGURE 1
(a) Geological setting of the captured bivalves. The height data were acquired from the ETOPO 2 database or the 1-minute global bathymetry/topography data from the M_map website. **(b)** Diagram of the experimental processes. **(c)** Photos showing the positions of carbonate powder acquisition via a hand-held dental drill. **(d)** Laser ablation inductively coupled plasma mass spectrometry (LA-ICP-MS) line scan of a thick section of the growth profile. As shown in Panel d, the scanning direction is from the umbo (oldest part of the shell) to the margin (youngest part of the shell).

therefore excluded from further analysis. IsoplotR was employed to further analyze the raw data (a free and open-source substitute for Ludwig's popular Isoplot add-in for Microsoft Excel) (Shangde et al., 1987). In calculation, the bulk earth $^{230}Th/^{232}Th$ activity ratio of 0.825 ± 50% was often used when the *in situ* data is difficult to obtain. A recent study demonstrated that the initial $^{230}Th/^{232}Th$ ratio for SCS cold-seep carbonates was 0.7 ± 0.1 (Wang et al., 2022), slightly different from the bulk earth value. However, in the context of this study, a unique local detritus value should be obtained by analyzing a modern sample to test assumptions regarding the initial Th and U isotopes.

2.3 Oxygen isotope analysis of growth profiles

The carbonate oxygen content was determined using a multi-line gas preparation and introduction device (GasBench-II) coupled with a stable isotope mass spectrometer (DELTA V Advantage) (GasBench-IRMS). First, a minimum of 50–100 ug of carbonate powder was drilled along the sample plate using a 50 diamond made of tungsten steel and placed it in a clean Labco reaction bottle (Wales, UK), the cap was tightened and placed on a thermostatic sample plate in sequence. Second, the purge air needle was fixed, the working procedure of the automatic sampler was set, and the sample bottle with He gas for up to 5 min in turn was emptied to remove the influence of the air in the bottle on the measurement of the sample O isotope ratio. Then, 8 drops of anhydrous phosphoric acid was added to the emptied sample bottle, which was heated on the dry thermostat for 70 °C for 1h. Finally, the sample was placed on an automatic sampler, the injection needle was fixed, and the abundance of CO2 (δ18O and δ16O) was measured via a mass spectrometer, and compared with that of the international standard substance (V-SMOW) to obtain the measured sample oxygen isotope ratio (δ value). To ensure the accuracy of the instrument and experimental results, the instrument is corrected first, and two carbonate standard samples (IAEA-CO-8 and IAEA-603) are added before and after each of the tested samples. The analytical accuracy of the δ18O value was ± 0.08 ‰. Specifically, the samples of mussels come from the inner and outer portions of the outer shell layer (iOSL, oOSL) because of the extremely thin layer of deep-sea mussels. For this purpose, we apply the two-component model to evaluate the potential bias of the oxygen isotopes and assign a value of -0.96 °C for temperature reconstruction of the two mussels.

2.4 Data processing

The high pressure, intense fluid with a relatively high seepage rate and potentially long life span make it more possible for diagenetic alteration to occur (Vernon and Clarke, 2008). Diagenetic alteration would cause a decrease in the trace elements contents, as well as more negative carbon and oxygen isotope values (Brand, 1980; Brand, 1981), and thus, would cause deviation from the temperature reconstruction. After high-pass filtering, we removed outliers based on a threshold of Mn/Sr ≥ 0.625 (Bruckschen et al., 1999; Korte et al., 2003). Then we applied the AR-detrending method according to reference methods to reconstruct the temperature (Brosset et al., 2023). The Ar method, or prewhitening, involves dividing the residuals from an AR model by their mean to produce a detrended series with a mean of 1 and white noise characteristics. This approach removes low-

TABLE 1 Analysis precision of LA-ICP-MS quality control using NIST SRM 610 and NIST SRM 612 as reference materials.

Reference material	NIST 610				NIST 612			
	Reference value [μg/g]	Deviation [%]	RSD [%]	LOD [μg/g]	Reference Value [μg/g]	Deviation [%]	RSD [%]	LOD [μg/g]
Li	468	0–0.2	0.1–1.0	0.9 ± 0.6	40.2	0.9–22.3	0.4–0.9	0.9 ± 0.5
Na	99415	0–0.2	0.1–0.9	4.2 ± 2.4	103858	0.4–22.5	0.2–0.6	4.1 ± 2.4
Mg	465	0–0.2	0.1–0.8	1 ± 0.7	68	8.5–24.8	0.3–0.7	1 ± 0.7
Ca	82144	0–0.2	0.1–0.6	151 ± 103.8	85049.3	1.2–16.9	0.2–0.4	148.6 ± 99.6
Mn	444	0–0.2	0.1–0.7	0.2 ± 0.1	38.7	0.7–17.0	0.2–0.6	0.2 ± 0.1
Fe	458	0–0.2	0.2–1.0	11.5 ± 8.4	51	1.5–97.0	0.6–4.3	11.4 ± 8.3
Cu	441	0–0.3	0.2–0.8	0.3 ± 0.2	37.8	0.2–22.6	0.4–0.8	0.3 ± 0.2
Zn	460	0–0.2	0.1–0.8	0.9 ± 0.4	39.1	0–19.9	0.3–0.8	0.9 ± 0.4
Sr	515.5	0–0.1	0.1–0.6	15.3 ± 15.2	78.4	1.5–17.4	0.2–0.8	19.2 ± 16.5
Mo	417	0–0.2	0.2–1.0	0.2 ± 0.2	37.4	0.8–23.0	0.4–0.9	0.2 ± 0.1
Ba	452	0–0.1	0.1–0.7	13.4 ± 13.4	39.3	1.3–13.9	0.3–0.6	18.5 ± 19.9
U	461.5	0–0.2	0.1–0.8	0.5 ± 0.5	37.38	0.1–18.3	0.3–0.6	0.3 ± 0.3

The average concentration ± standard deviation is given in μg/g. Reference values are taken from the GeoReM database (http://georem.mpch-mainz.gwdg.de/). Unstable data are highlighted in yellow color.

frequency variations, retaining only high-frequency fluctuations. The temperature range of the cultivation experiment was similar to that of the cold seeps.

3 Results and discussion

3.1 Potential sources and subject processes affecting trace elements concentration in cold seep bivalves

As is shown in Figure 2a, there exists no orthogonal relationship. If physiological processes are induced by environmental change, the physiological changes could ultimately be explained as a component of environmental changes. If physiological changes were not related to environmental changes, they should present an orthogonal relationship. Clearly, orthogonal elements were not observed in this study (Figure 2a). Therefore, the heterogeneous element distribution could be explained by the environmental variables. The results also demonstrated that two main principal components (PCs) cumulatively explained 60.8% of the variance in the dataset, suggesting that the two PCs could partly explain the patterns of the M/Ca ratios (Figure 2b). Results showed significant difference ($P < 0.001$) among the Li/Ca, Na/Ca, Mg/Ca, Mn/Ca and U/Ca ratios in the mussels collected from the F site (Figure 3). At the HM site, significant differences were found among Li/Ca, Na/Ca, Ba/Ca and U/Ca ratios in the mussels with different sizes, whereas the Na/Ca, Mn/Ca, Ba/Ca and U/Ca ratios also differed significantly for clams. This demonstrated the highly heterogeneous distribution of trace elements in cold seep bivalves even if they were collected from the same site. Such heterogeneity might result from physiological processes and environmental variables such as temperature, salinity, acidity and redox conditions. We inferred that physiological processes could be neglected which could be supported by principal component analysis.

The first PC showed that the loading for the Sr/Ca ratio was -0.04, whereas the values for the remaining elements ranged from 0.18 to 0.42 (Figure 2c). The relatively low loadings suggest that the Sr/Ca ratio tends to be controlled by relatively stable environmental variables such as temperature and salinity. A previous study indicated that very slight changes (~ 0.8%) in the partition coefficient for Sr were observed when the salinity increased per unit within the range of 20 – 40 PSU (Dodd and Crisp, 1982). Moreover, Poulain et al. demonstrated that the Sr/Ca ratio tends to remain constant when the salinity exceeds 35 PSU (Poulain et al., 2015). Accordingly, salinity did not influence the Sr/Ca ratio in the cold seep (PSU~35), instead, this ratio was more likely dependent on the temperature. This could be supported by a recent study that revealed a significant correlation between the Sr/Ca ratio and

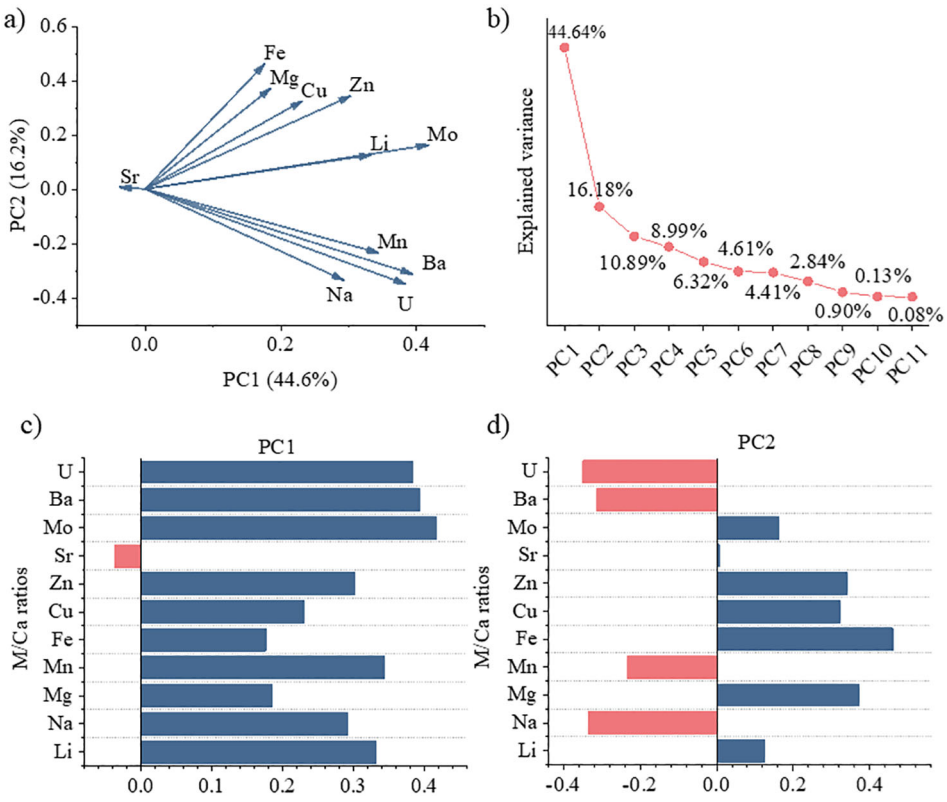

FIGURE 2
(a) Principal component analysis (PCA) plot of the M/Ca ratios of each shell. The projection of each element on the axis is the score on that axis, indicating its importance. Acute angles between different element arrows indicate positive relationships between them. **(b)** Variance of each principal component. **(c)** PCA loadings of each M/Ca for PC1. **(d)** PCA loadings of each M/Ca for PC2. All M/Ca ratios are shown in the form of M in short in all the graphs.

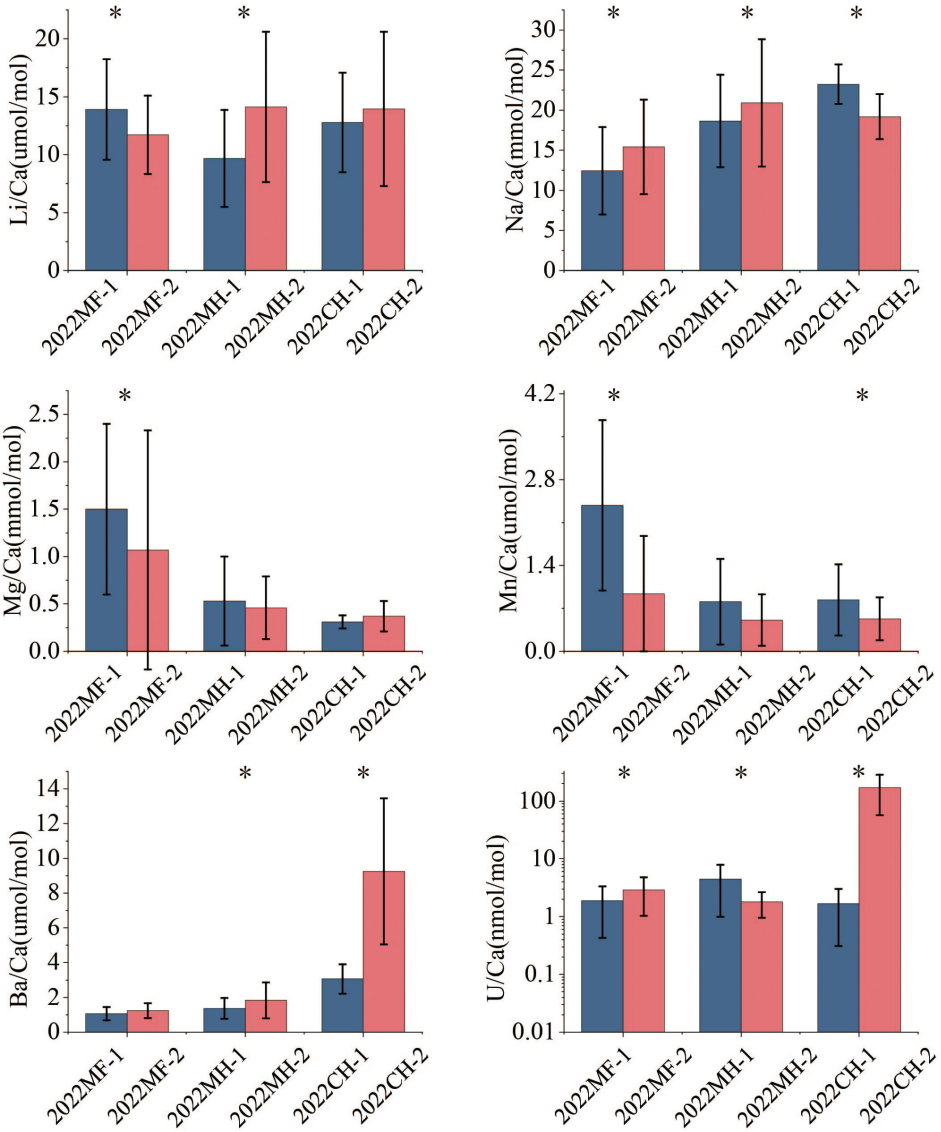

FIGURE 3
Element (M)/calcium (Ca) ratios measured in bivalves of different sizes. Asterisk represents the data with significant differences via Tukey's test ($P < 0.001$). The blue color stand for samples with smaller size while red color for bigger size within the same location.

temperature, while the correlation coefficient could be highly improved via detrending method to eliminate the physiological trend (Brosset et al., 2023).

Similarly, the loading of the Sr/Ca ratio was also the lowest (~ 0.006) among all the elements for the second PC (Figure 2d). Negative loadings were found for U/Ca, Ba/Ca, Mn/Ca and Na/Ca. The loadings were similar for Na/Ca, U/Ca and Ba/Ca and these element ratios could serve as potential acidification proxies. For example, Zhao et al. revealed that marine acidification adaptation could be achieved through a Na^+/H^+ exchange pump where a lower pH (more specifically, pCO_2) led to a higher Na/Ca ratio. U/Ca serves as an indicator of the carbonate system, showing a negative relationship with $[CO_3^{2-}]$ and thus a positive relationship with acidification (Raitzsch et al., 2011). When the pH decreased, soluble bicarbonate increased which increased the concentration of soluble U in the form of uranyl mono-carbonate. In the context of this study, the increase in the Ba/Ca ratio was unlikely to be influenced by phytoplankton, such as that in the freshwater counterpart because the chlorophyll content was not found in the cold seep seafloor (Fröhlich et al., 2022; Di et al., 2023). Instead, the dissolved Ba in the pore fluids was produced mainly from the anaerobic oxidation of methane (AOM) which consumed SO_4^{2-} and decreased the pH by generating H_2S (Torres et al., 2001, 2003). Additionally, the effects of the seepage intensity on the Mn/Ca ratio should be similar to those on the above three elements since they all had negative loadings (Figure 4d). The increase in the seepage intensity decreased the pH and dissolved oxygen content, which increased the Mn/Ca ratio, as a previous study demonstrated that the Mn/Ca ratio was negatively correlated with the dissolved oxygen content after physiological bias was eliminated through detrending

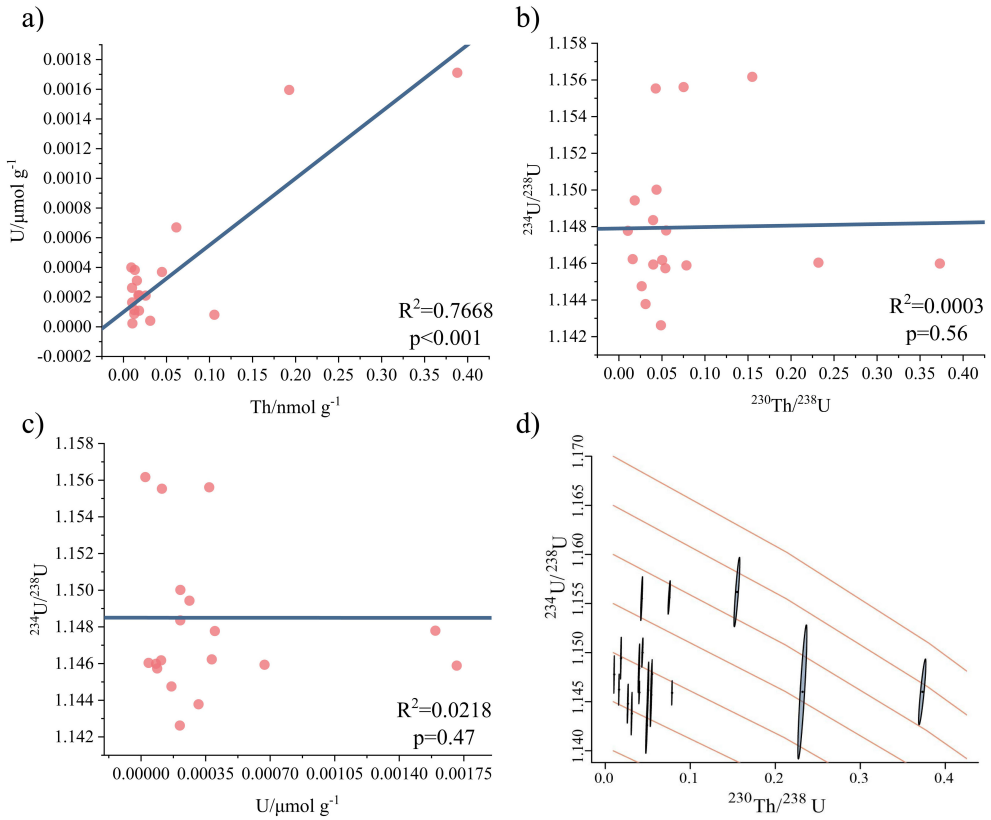

FIGURE 4
(a) Plot of uranium (U) versus thorium (Th) concentrations. **(b)** Plot of $^{234}U/^{238}U$ versus $^{230}Th/^{238}U$. **(c)** U plotted against $^{234}U/^{238}U$. **(d)** Plot of all sample data for $^{234}U/^{238}U$ versus $^{230}Th/^{238}U$, with all the plotted points lying along the marine evolution line (1.147 ± 0.015).

(Schöne et al., 2021). The redox conditions also change with the increasing seepage intensity, promoting the release of Mn from the sediment into the water (Millward et al., 1998). The concentration of Mn in the shell tends to increase, as it is proportional to that in the ambient water (Freitas et al., 2006).

Moreover, PC2 shows different trends under seepage. Positive loadings were found for Li/Ca, Mg/Ca, Fe/Ca, Cu/Ca, Zn/Ca, and Mo/Ca for the second PC, indicating a decreasing tendency in these element ratios if the seepage intensity increased. The values of these ratios are influenced by two competitive processes including digestion and precipitation. Bacteria could use Fe-Mn oxides, Mo, and enzymatic cofactors consisting of Mo and Cu during methane-oxidizing reactions (Beal et al., 2009; Glass et al., 2014), which eventually increase the concentration of these elements in the shell. On the other hand, these trace elements tend to precipitate, reducing their concentration in the water and shell in a higher degree of redox condition. According to our results, the predominant process influencing the concentration of these elements was precipitation rather than bypass flow from digestion. Nevertheless, the precipitation mechanisms differ among these elements. For example, Mo, Fe, Cu and Zn coprecipitate with H_2S under redox conditions (Hu et al., 2015). Li precipitation was due to deep-seated diagenetic processes where Li in deeply buried continental margin sediments was conveyed to shallow sediments and sequestrated by secondary minerals due to the lower temperatures that prevail in diagenetic environments (Berger et al., 1988; James and Palmer, 2000; James et al., 2003; Scholz et al., 2010). Mg tends to precipitate under increasing seepage, because all the seepage-related reactions (sulfate reduction, AOM, and methanogenesis) can generate HCO_3^- (Meister and Reyes, 2019). It should be noted that these elements could not be released into the water column once they precipitated because they were not redox-sensitive elements such as Mn. Moreover, diffusion and resuspension cannot supply additional ion concentrations under redox conditions.

Overall, the results of the PCA highlighted the different subject factors for the trace elements associated with seepage. Sr was dependent mainly on relatively constant environmental variables such as temperature. U, Ba, and Na are subject to acidification process, whereas Mn is predominantly controlled by redox conditions (i.e., dissolved oxygen). For the remaining elements including Li, Fe, Cu, Mg, Zn and Mo, precipitation was the critical process dominating their concentration in the cold seep shell.

3.2 Median ages of cold seep bivalves estimated by u-series dating

To evaluate the validity of the U-series dating approach for estimating the age of cold seep bivalves, we tested the $^{234}U/^{238}U$ ratio, a parameter for back-calculation of the initial U isotope ratio during bivalve growth after determining an age (Edwards et al., 2003),

to confirm whether the shell was a closed system because the correction method was simpler and the error of the calculated age was smaller in a closed system. The results demonstrated that the $^{234}U/^{238}U$ ratio was within that of the present-day water (i.e. 147‰ ± 15‰) (Figure 4b), indicating that it tends to be a closed system otherwise the value of this parameter would be abnormally high. This was further supported by determining whether the alpha-recoil processes took place which resulted in the microscale redistribution of daughter isotopes from recoil-damaged lattice sites[58]. Isotopic redistributions would result in positive correlations between $^{230}Th/^{238}U$ and $^{234}U/^{238}U$, leading to discrepancies between calculated and actual ages that increase over time. Our results demonstrated a very poor relationship between $^{234}U/^{238}U$ and $^{230}Th/^{238}U$ (R^2 = 0.0003), suggesting the absence of alpha-recoil processes.

To further confirm that the shell was a closed system without alpha-recoil processes and correct the results, we used three models proposed by Thompson et al., Villemant and Feuillet, and Scholz et al. to assess the potential contribution of alpha-recoil processes to the calculated age errors (Thompson et al., 2003; Villemant and Feuillet, 2003; Scholz et al., 2004; Frank et al., 2006). The results indicated that these three models were not applicable to the cases in the present study because negative values were obtained in the calculated ages using the first two models. The abnormally high values of more than 1000 years were observed via the Scholz model. This finding might be attributed to the specific assumptions of these models. For example, the Villemant and Feuillet model assumes an initial excess of ^{230}Th and the continuous selective redistribution of ^{234}U, ^{234}Th, and ^{230}Th. The Thompson model assumes the simultaneous adsorption of particle-reactive ^{234}Th and ^{230}Th in the shell. The Scholz model assumes a proportional loss of U during the uptake process in the shell. These assumptions are basic indications of alpha-recoil processes; therefore, the alpha-recoil process was not the predominant source of the age errors in this study.

Another possible source of errors might be Th contamination. As shown in Table 2. Uranium-thorium dating details for each shell. The U concentration errors for modern shells are <0.001. The corrected $\delta^{234}U$ and calculated ages were determined using the $^{230}Th/^{232}Th$ from the margins as the initial $^{230}Th/^{232}Th$ ratio, assuming that it remains constant for a short time. The measured $^{230}Th/^{232}Th$ activity ratio was extremely low (1.331 ± 0.306) with very high excess Th, which indicating a high degree of Th contamination. The results also indicated that Th contamination resulted mainly from the life habits of cold seep bivalves rather than the U uptake. Although a significant correlation (R^2 = 0.7668, $P < 0.01$) was observed between U and Th, the correlation became insignificant ($P > 0.01$) if the two data with high Th contents (24.512 ppb and 90 ppb for 2022CH-2 and 2022CH-3, respectively) were removed. This demonstrated that the increase of Th concentration did not depend on U adsorption, suggesting different uptake patterns for U and Th. The marine carbonate U mainly originates from seawater as the $^{234}U/^{238}U$ ratio is within 15‰ of 147‰ which is the signature of modern seawater (Henderson, 2002) (Table 2).

TABLE 2 Uranium-thorium dating details for each shell.

Shell i.d.	Height	Part	^{238}U (ppm)	^{232}Th (ppb)	$^{230}Th/^{232}Th$	$^{230}Th/^{238}U$	$^{234}U/^{238}U$	Calculated age (a)
2022MF-1	55.1	Umbo	0.062	2.322 (4)	1.499 (34)	0.0184 (4)	1.1494 (17)	327 ± 39
		Margin	0.039	2.325 (3)	1.353 (25)	0.0265 (5)	1.1448 (16)	Modern
2022MF-2	79.7	Umbo	0.074	3.608 (6)	1.932 (33)	0.0310 (5)	1.1438 (17)	1111 ± 49
		Margin	0.021	2.911 (7)	1.164 (20)	0.0540 (9)	1.1457 (26)	Modern
2022MF-3	106.1	Umbo	0.095	2.124 (4)	1.412 (41)	0.0104 (3)	1.1478 (15)	132 ± 28
		Margin	0.027	2.940 (4)	1.185 (26)	0.0428 (9)	1.1555 (18)	Modern
2022MH-1	93.3	Umbo	0.159	14.262 (24)	1.354 (15)	0.0399 (5)	1.1459 (9)	394 ± 43
		Margin	0.051	4.032 (6)	1.664 (24)	0.0437 (6)	1.1500 (12)	Modern
2022MH-2	115.9	Umbo	0.088	10.376 (20)	1.932 (28)	0.0752 (11)	1.1556 (14)	2767 ± 103
		Margin	0.050	5.964 (12)	1.242 (25)	0.0488 (10)	1.1426 (23)	Modern
2022MH-3	122.1	Umbo	0.091	3.049 (4)	1.453 (25)	0.0160 (3)	1.1462 (13)	253 ± 29
		Margin	0.051	4.228 (6)	1.440 (28)	0.0397 (8)	1.1484 (20)	Modern
2022CH-1	106.6	Umbo	0.026	4.200 (8)	0.937 (16)	0.0502 (8)	1.1462 (23)	Modern
		Margin	0.010	7.205 (23)	0.949 (17)	0.2319 (43)	1.1460 (55)	Modern
2022CH-2	130.0	Umbo	0.380	44.695 (7)	1.416 (19)	0.0549 (28)	1.1478 (28)	Modern
		Margin	0.407	90.00 (52)	1.077 (8)	0.0784 (35)	1.1459 (27)	Modern
2022CH-3	140.2	Umbo	0.005	2.405 (82)	1.067 (9)	0.1549 (3)	1.1562 (12)	Modern
		Margin	0.019	24.512 (130)	0.890 (4)	0.3729 (3)	1.1460 (10)	Modern

The corrected $\delta^{234}U$ and calculated ages were determined using the $^{230}Th/^{232}Th$ from the margins as the initial $^{230}Th/^{232}Th$ ratio, assuming that it remains constant for a short time. The U concentration errors for modern shells are <0.001.

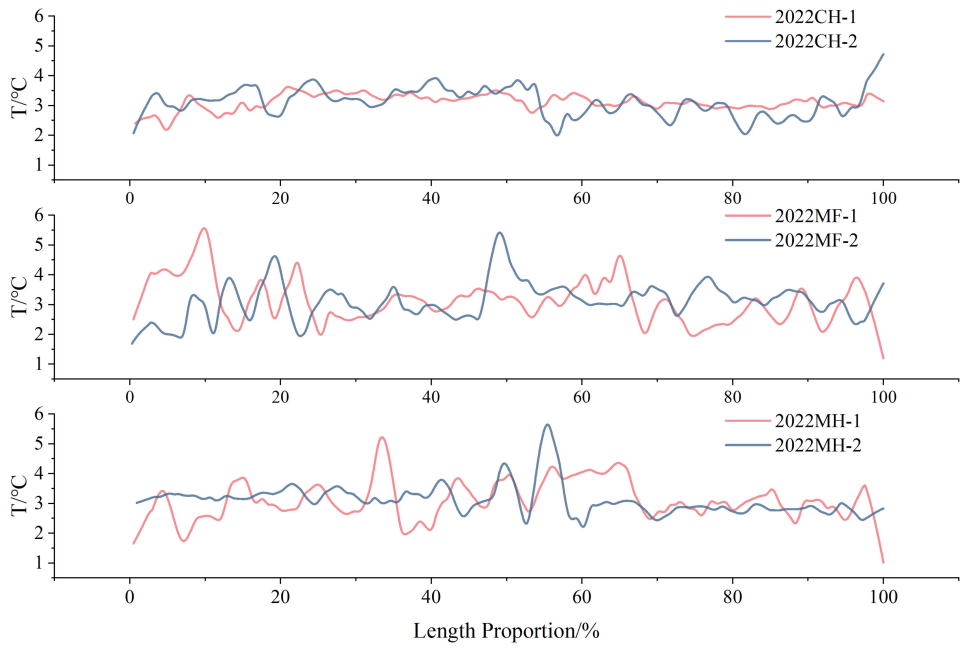

FIGURE 5
Temperature reconstruction based on the detrended strontium/calcium ratio. The x-axis displays the height proportion normalized to 0 - 100% where 0 and 100% represent the oldest and youngest parts of the shell, respectively. Bivalves in different locations might not grow at the same rate.

As suggested by Wang et al (Wang et al., 2022), Th contamination in cold seep carbonate mainly originates from detritus due to the contributions of Fe-Mn oxides and organic matter. Our results demonstrated that the aforementioned two abnormal data sets (i.e., 2022CH-2 and 2022CH-3) contained high concentrations of Fe, Mn and Mg. Accordingly, it was inferred that detritus might be the main contributor of Th contamination. Samples such as the clams collected from the BGB site belong to the group of *A. marissinica*, which mostly feeds on sulfide-oxidizing bacteria and reaches its foot deep into the sediment to obtain sulfide energy (Feng et al., 2018). During this process, it may contact and adsorb detritus in the sediment, which eventually leads to a high content of Th in the shell.

Accordingly, we used the initial $^{230}Th/^{232}Th$ activity ratio to correct the calculation and minimize the effects of Th contamination on the results. Generally, a bulk earth $^{230}Th/^{232}Th$ activity ratio of 0.825 ± 50% was often used when the *in situ* data is difficult to obtain. A recent study demonstrated that the initial $^{230}Th/^{232}Th$ ratio for SCS cold-seep carbonates was 0.7 ± 0.1 (Wang et al., 2022). In the context of this study, a unique local detritus value should be obtained by analyzing a modern sample to test assumptions regarding the initial Th and U isotopes. The results of the isochron analysis (MSWD < 1, $P > 0.05$) of the modern margin samples showed that the values of initial $^{230}Th/^{232}Th$ values were stable at each cold seep site which varied insignificantly between the F and Haima sites. Therefore, an average value of 1.218 ± 0.008 was used to correct the calculation and the results are listed in Table 2. For the Haima clams, the calculated age was only 0.000056 years. This suggested that these clam samples were too young to be dated via the typical U-series dating approach, because this method relies on the decay of U to Th which might not occur sufficiently in such a short timeframe to be measurable. Accordingly, it was inferred that the median age of Haima clams was less than 100 years. For the cold-seep mussels, the calculated age ranged from 132 to 394 years with only two age anomalies up to thousands of years observed in the 2022MF-2 and 2022MH-2 samples. As mentioned above, the age bias in these two samples might be caused by the uncertainty of Th detritus based on the long-term constant assumption instead of anomalous $\delta^{234}U$ due to diagenesis. *The acceptance of a stricter predefined range falling within modern seawater is recommended to exclude the samples with potential age bias* (Gallup et al., 1994). *In this paper, when a stricter rule of $\delta^{234}U$ falling within 2.5‰ of 147‰ was applied, two abnormal samples (i.e., 2022MF-2 and 2022MH-2) could be excluded.* In this case, the median ages of 229.5 and 323.5 years were assigned to the mussels from F and HM sites, respectively. The estimated age of the cold seep bivalves was one-order magnitude greater than that of the freshwater bivalves. This finding agrees with previous results obtained from the 228Ra chronology dating method which demonstrated that the deep-sea bivalves can live for up to 100 years (Turekian et al., 1975). It can be concluded that the cold seep bivalves could serve as long-lived geological proxies for investigating the long-term evolution of cold seep environments.

3.3 Reconstruction of the environments of cold seep bivalves

Cold seeps exhibit remarkable diversity as continental margin habitats. Various factors contribute to the heterogeneity of these ecosystems, including distinct fluid flow patterns, geochemical variations, and diverse substrate types (Cordes et al., 2010). Such

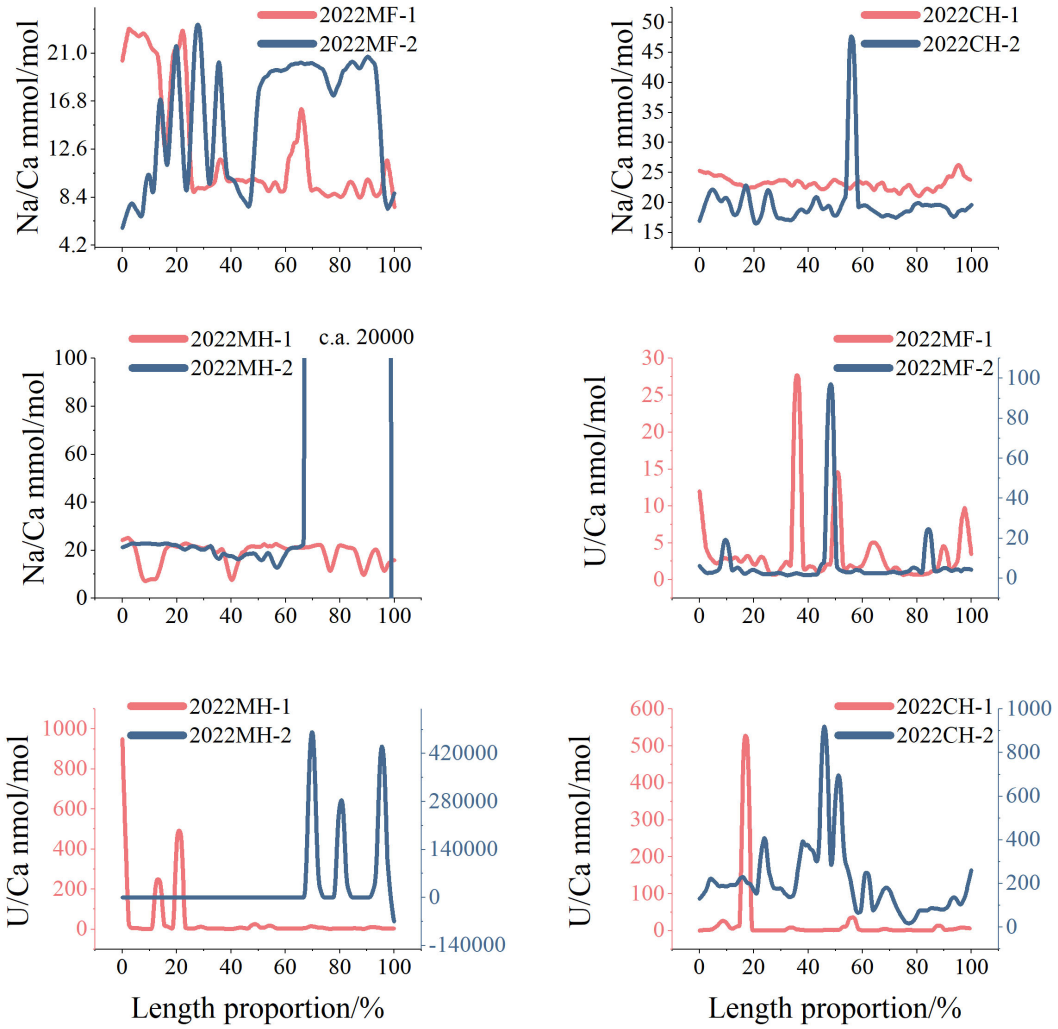

FIGURE 6
Profiles of the sodium/calcium and uranium/calcium ratios. The data were smoothed via the LOWESS method with a window ratio of 0.05.

abiotic sources of heterogeneity foster the development of unique microbial communities, foundation species hosting microbial symbionts, and a wide range of associated heterotrophic species (Cordes et al., 2010). This can lead to discrepancies in samples acquired from the same site. For this reason, the elements related to local fluid conditions were excluded from the analysis, whereas the oxygen isotopes, Sr/Ca, Na/Ca and U/Ca were selected for reconstructing the key parameters of the cold seep environment such as temperature and acidification.

First, verification of whether the oxygen isotopes can be employed to reconstruct cold seep temperatures is needed. An early study demonstrated a significant correlation between oxygen and carbon isotopes in present day bivalve shells from hydrothermal vents, which could reflect the relationship between increased temperature and the seepage of CO_2 and CH_4 containing depleted $\delta^{13}C$ (Rio et al., 1992). However, a statistical correlation was not detected between oxygen and carbon isotopes in the present study, even when they were detrended via a high-pass filter at 0.125 Hz. In this study, the oxygen isotopes for 2022CH-1 and 2022CH-2 were 4.14 ± 0.14‰ and 5.19 ± 1.23‰, respectively. According to Lécuyer et al, the oxygen isotope fractions between biogenic aragonite and water is approximately 2–3‰ (Lécuyer et al., 2012). Even when this value was subtracted, the oxygen isotopes in the shell were still higher than those in the ambient water. The more positive values of oxygen isotopes in the cold-seep shells might be associated with the pore water chemistry and seepage intensity in the presence of methane hydrate. Similar to the water freezing process, the conversion of liquid water to solid methane hydrates leads to isotopic fractionation, enriching heavy isotopes within the solid structure. Since the dissociation pressure of a lattice form of heavy isotopes was lower than that of a lattice composed of light isotopes, the solid hydrate preferred to incorporate heavier isotopes, leaving lighter isotopes in the surrounding water (Trofimuk et al., 1974). This could be supported by a previous study that demonstrated that pore water $\delta^{18}O$ was enriched in surface sediments. These findings suggest that oxygen isotope anomalies in the pore water could affect bivalves although they can form shells from minerals in ambient water, which increasing the error in temperature calculations based on oxygen

isotopes. However, to the best of our knowledge, oxygen isotope information in cold-seep environments is very limited in the literature, making reconstructing temperatures on the basis of oxygen isotopes in cold-seep environments very difficult.

Nevertheless, a negative correlation was observed between the raw $\delta^{13}C$ values and the temperature calculated from the Sr/Ca ratio ($P < 0.001$), indicating that the Sr/Ca ratio reflected the temperature change synchronously with changes in carbon isotopes better than the changes of oxygen isotopes. Combined with the significant dependence of the Sr/Ca ratio on temperature revealed by aforementioned PCA, we believe that the Sr/Ca ratio could serve as a reliable proxy for the cold seep environment temperature. The temperature reconstructed from the Sr/Ca ratio ranged from 1 to 6°C with small fluctuations (Figure 5). Unlike in other seafloors, the temperature estimated in cold seeps did not increase with time, and in most cases, the temperature was lower than the background value for the seafloor temperature in the South China Sea (i.e., 5 °C). This agreed with a previous study in which the cooling effects resulting from CO_2 uptake overwhelmed the warming effects from the emitted heat and greenhouse gases (Pohlman et al., 2017).

In addition, we also attempted to reconstruct cold seep acidification using Na/Ca and U/Ca as candidate proxies, considering their potential correlations to CO_2 and $[CO_3^{2-}]$, respectively from aforementioned PCA. Figures 6a-c show the temporal evolution of Na/Ca. The largest degree of fluctuation was noticed in the F site where the Na/Ca ratio ranged from 6 to 24 mmol/mol with irregular pattern (Figure 6a). The Na/Ca ratios in the samples from 2022CH-1 and 2022CH-2 slightly fluctuated around 20 and 23 mmol/mol, respectively, but one abnormally high value exceeding 45 mmol/mol appeared in 2022CH-2 (Figure 6c). This tendency was more obvious in 2022MH-2 where an extremely high value of c.a. 20000 mmol/mol was observed (Figure 6b). The appearance of abnormally high values might be attributed to the metabolic disturbance caused by changes in environmental conditions. For example, an increase in the environmental temperature can alter the cell membrane permeability and increase the energy costs required to maintain alkaline conditions in the extrapallial fluid (Zhao et al., 2017a). This mechanism can suppress the activities of enzymes involved in the synthesis of the organic matrix and changed the acidification until the pH exceeding the tolerance limits (Zhao et al., 2017a). Compared with that of Na/Ca, the baseline of U/Ca was much flatter, and more flats and abnormally high values appeared (Figures 6d-f). However, the detailed mechanisms underlying the response of Na/Ca and U/Ca to acidification remain unclear at the current stage, demanding that future studies to validate the feasibility of using these two trace elements as acidification proxies before practical application.

4 Conclusions

This study investigated the biochemical characteristics of the growth profiles of cold seep bivalves and estimated the median age via the U-series dating method. This demonstrated that the shell was a closed system and that the bias in U-Th dating was primarily due to the low initial $^{230}Th/^{232}Th$ rather than alpha-recoil processes. After the age was corrected by the margin $^{230}Th/^{232}Th$ ratio as the initial $^{230}Th/^{232}Th$ ratio and the anomaly was excluded by applying the criterion of falling within 2‰ of 147‰, the respective median values of 229.5 and 323.5 years were allocated to the mussels collected from the F and HM sites. The median age of Haima clams was inferred to be less than 100 years. Cold seep bivalves can serve as a potential proxy in addition to foraminifer. Moreover, this study suggested different uptake mechanisms for the trace elements associated with seepage: Sr is mainly controlled by temperature changes. U, Ba, and Na are subject to acidification, whereas Mn is predominantly controlled by redox conditions, especially for the dissolved oxygen. For the remaining elements, including Li, Fe, Cu, Mg, Zn and Mo, precipitation was the critical process dominating their concentration in the cold seep shell. Through combined analysis, Sr/Ca was identified as a proxy for cold seep temperature reconstruction rather than the oxygen isotopes. Accordingly, the temperature reconstructed from the Sr/Ca ratio ranged from 1 to 6°C with small fluctuations and did not show a warming trend. Although Na/Ca and U/Ca are potentially linked to the concentrations of dissolved CO_2 and $[CO_3^{2-}]$, they can only be used as promising proxies for reconstructing cold seep acidification after eliminating unknown bias. Overall, this study suggests uranium-series dating as well as trace elements in cold seep bivalves as new prospects to reconstruct the hundred-year-scale evolution of deep-sea temperature in the future.

Data availability statement

The original contributions presented in the study are included in the article/supplementary material. Further inquiries can be directed to the corresponding author.

Author contributions

CC: Writing – original draft, Writing – review & editing. JF: Writing – review & editing. GW: Writing – review & editing. RH: Writing – review & editing. XC: Writing – review & editing. JL: Writing – review & editing. XZ: Writing – original draft. SZ: Writing – original draft.

Funding

The author(s) declare that financial support was received for the research and/or publication of this article. Financial support was received from the National Natural Science Foundation of China (42325603, 42227803, 42376215, 42206223), the National Key Research and Development Program of China (2021YFF0502300), Guangdong Natural Resources Foundation (GDNRC(2023)30),and the PI project of Southern Marine Science and Engineering Guangdong Laboratory (Guangzhou) (GML20190609, GML2022009, and GML20230921).

Acknowledgments

We are grateful to the crew of the scientific research vessel (R/V) KEXUE (Institute of Oceanology, Chinese Academy of Sciences, China) for their assistance in collecting the samples.

Conflict of interest

The authors declare that the research was conducted in the absence of any commercial or financial relationships that could be constructed as a potential conflict of interest.

Generative AI statement

The author(s) declare that no Generative AI was used in the creation of this manuscript.

Publisher's note

All claims expressed in this article are solely those of the authors and do not necessarily represent those of their affiliated organizations, or those of the publisher, the editors and the reviewers. Any product that may be evaluated in this article, or claim that may be made by its manufacturer, is not guaranteed or endorsed by the publisher.

References

Barrat, J.-A., Chauvaud, L., Olivier, F., Poitevin, P., and Rouget, M.-L. (2023). Trace elements in bivalve shells: How "vital effects" can bias environmental studies. *Chem. Geol.* 638, 121695. doi: 10.1016/j.chemgeo.2023.121695

Beal, E. J., House, C. H., and Orphan, V. J. (2009). Manganese- and iron-dependent Marine methane oxidation. *Science* 325. doi: 10.1126/science.1169984

Berger, G., Schott, J., and Guy, C. (1988). Behavior of Li, Rb and Cs during basalt glass and olivine dissolution and chlorite, smectite and zeolite precipitation from seawater: experimental investigations and modelization between 50 and 300 °C. *Chem. Geol.* 71, 297–312. doi: 10.1016/0009-2541(88)90056-3

Biló, T. C., Perez, R. C., Dong, S., Johns, W., and Kanzow, T. (2024). Weakening of the Atlantic Meridional Overturning Circulation abyssal limb in the North Atlantic. *Nat. Geosci.* 1-7. doi: 10.1038/s41561-024-01422-4

Boetius, A., and Wenzhöfer, F. (2013). Seafloor oxygen consumption fuelled by methane from cold seeps. *Nat. Geosci.* 6, 725–734. doi: 10.1038/ngeo1926

Brand, U. V. J. (1980). Chemical diagenesis of a multicomponent carbonate system; 1, Trace elements. *J. Sediment. Res.* 50, 1219–1236. doi: 10.1306/212F7BB7-2B24-11D7-8648000102C1865D

Brand, U. V. J. (1981). Chemical diagenesis of a multicomponent carbonate system; 2, Stable isotopes. *J. Sediment. Res.* 51, 987–997. doi: 10.1306/212F7DF6-2B24-11D7-8648000102C1865D

Brosset, C., Höche, N., Witbaard, R., Nishida, K., Shirai, K., Mertz-Kraus, R., et al. (2023). Sr/Ca in shells of laboratory-grown bivalves (*Arctica islandica*) serves as a proxy for water temperature–implications for (paleo) environmental research? *Front. Mar. Sci.* 10, 1279164. doi: 10.3389/fmars.2023.1279164

Bruckschen, P., Oesmann, S., and Veizer, J. (1999). Isotope stratigraphy of the European Carboniferous: proxy signals for ocean chemistry, climate and tectonics. *Chem. Geol.* 161, 127–163. doi: 10.1016/S0009-2541(99)00084-4

Ceramicola, S., Dupré, S., Somoza, L., and Woodside, J. (2018). Cold seep systems. *Submar. geomorphol.*, 367–387. doi: 10.1007/978-3-319-57852-1_19

Chen, T., Robinson, L. F., Li, T., Burke, A., Zhang, X., Stewart, J. A., et al. (2023). Radiocarbon evidence for the stability of polar ocean overturning during the Holocene. *Nat. Geosci.* 16, 631–636. doi: 10.1038/s41561-023-01214-2

Cheng, H., Adkins, J., Edwards, R. L., and Boyle, E. A. (2000). U-Th dating of deep-sea corals. *Geochim. Cosmochim. Acta* 64, 2401–2416. doi: 10.1016/S0016-7037(99)00422-6

Cordes, E. E., Cunha, M. R., Galéron, J., Mora, C., Olu-Le-Roy, K., Sibuet, M., et al. (2010). The influence of geological, geochemical, and biogenic habitat heterogeneity on seep biodiversity. *Mar. Ecol.* 31, 51–65. doi: 10.1111/j.1439-0485.2009.00334.x

Di, P., Li, N., Chen, L., Feng, J., and Chen, D. (2023). Elevated nutrients and surface chlorophyll-α associated with natural methane seeps in the Haima cold seep area of the Qiongdongnan Basin, northern South China Sea. *Mar. pollut. Bull.* 191, 114873. doi: 10.1016/j.marpolbul.2023.114873

Dodd, J. R., and Crisp, E. L. (1982). Non-linear variation with salinity of Sr/Ca and Mg/Ca ratios in water and aragonitic bivalve shells and implications for paleosalinity studies. *Palaeogeogr. Palaeoclimatol. Palaeoecol.* 38, 45–56. doi: 10.1016/0031-0182(82)90063-3

Dutton, A. (2015). "Uranium-thorium dating," in *Handbook of sea-level research*, 386–403. doi: 10.1002/9781118452547

Edwards, R. L., Gallup, C. D., and Cheng, H. (2003). Uranium-series dating of marine and lacustrine carbonates. *Rev. Mineral. Geochem.* 52, 363–405. doi: 10.2113/0520363

Feng, D., Qiu, J.-W., Hu, Y., Peckmann, J., Guan, H., Tong, H., et al. (2018). Cold seep systems in the South China Sea: An overview. *J. Asian Earth Sci.* 168, 3–16. doi: 10.1016/j.jseaes.2018.09.021

Frank, N., Turpin, L., Cabioch, G., Blamart, D., Tressens-Fedou, M., Colin, C., et al. (2006). Open system U-series ages of corals from a subsiding reef in New Caledonia: Implications for sea level changes, and subsidence rate. *Earth Planet. Sci. Lett.* 249, 274–289. doi: 10.1016/j.epsl.2006.07.029

Freitas, P. S., Clarke, L. J., Kennedy, H., Richardson, C. A., and Abrantes, F. (2006). Environmental and biological controls on elemental (Mg/Ca, Sr/Ca and Mn/Ca) ratios in shells of the king scallop *Pecten maximus*. *Geochim. Cosmochim. Acta* 70, 5119–5133. doi: 10.1016/j.gca.2006.07.029

Fritz, L. W. (2001). Chapter 2 Shell structure and age determination. *Develop. Aquacult. Fish. Sci.* 31, 53–76. doi: 10.1016/S0167-9309(01)80030-2

Fröhlich, L., Siebert, V., Huang, Q., Thébault, J., Jochum, K. P., and Schöne, B. R. (2022). Deciphering the potential of Ba/Ca, Mo/Ca and Li/Ca profiles in the bivalve shell *Pecten maximus* as proxies for the reconstruction of phytoplankton dynamics. *Ecol. Indic.* 141, 109121. doi: 10.1016/j.ecolind.2022.109121

Füllenbach, C. S., Schöne, B. R., and Mertz-Kraus, R. (2015). Strontium/lithium ratio in aragonitic shells of *Cerastoderma edule* (Bivalvia) — A new potential temperature proxy for brackish environments. *Chem. Geol.* 417, 341–355. doi: 10.1016/j.chemgeo.2015.10.030

Gallup, C. D., Edwards, R. L., and Johnson, R. G. (1994). The timing of high sea levels over the past 200,000 years. *Science* 263, 796–800. doi: 10.1126/science.263.5148.796

Gilkinson, K. D. (1986). Shell microstructure and observations on internal banding patterns in the bivalves *Yoldia thraciaeformis* STORER 1838, and *Nuculana pernula* MULLER 1779 (Nuculanidae), from a deep-sea environment. *Veliger* 29, 70–77.

Gillikin, D. P., and Dehairs, F. (2013). Uranium in aragonitic marine bivalve shells. *Palaeogeogr. Palaeoclimatol. Palaeoecol.* 373, 60–65. doi: 10.1016/j.palaeo.2012.02.028

Glass, J. B., Yu, H., Steele, J. A., Dawson, K. S., Sun, S., Chourey, K., et al. (2014). Geochemical, metagenomic and metaproteomic insights into trace metal utilization by methane-oxidizing microbial consortia in sulphidic marine sediments. *Environ. Microbiol.* 16, 1592–1611. doi: 10.1111/emi.2014.16.issue-6

Groeneveld, J., Ho, S. L., Mackensen, A., Mohtadi, M., and Laepple, T. (2019). Deciphering the variability in Mg/Ca and stable oxygen isotopes of individual foraminifera. *Paleoceanogr. Paleoclimatol.* 34, 755–773. doi: 10.1029/2018PA003533

Halary, S., Riou, V., Gaill, F., Boudier, T., and Duperron, S. (2008). 3D FISH for the quantification of methane-and sulphur-oxidizing endosymbionts in bacteriocytes of the hydrothermal vent mussel *Bathymodiolus azoricus*. *ISME J.* 2, 284–292. doi: 10.1038/ismej.2008.3

Hart, S. R., and Blusztajn, J. (1998). Clams as recorders of ocean ridge volcanism and hydrothermal vent field activity. *Science* 280, 883–886. doi: 10.1126/science.280.5365.883

Henderson, G. M. (2002). Seawater (234U/238U) during the last 800 thousand years. *Earth Planet. Sci. Lett.* 199, 97–110. doi: 10.1016/S0012-821X(02)00556-3

Hu, Y., Feng, D., Liang, Q., Xia, Z., Chen, L., and Chen, D. (2015). Impact of anaerobic oxidation of methane on the geochemical cycle of redox-sensitive elements at cold-seep sites of the northern South China Sea. *Deep Sea Res. Part II: Topical Stud. Oceanogr.* 122, 84–94. doi: 10.1016/j.dsr2.2015.06.012

James, R. H., Allen, D. E., and Seyfried, W. E. Jr. (2003). An experimental study of alteration of oceanic crust and terrigenous sediments at moderate temperatures (51 to 350 C): Insights as to chemical processes in near-shore ridge-flank

hydrothermal systems. *Geochim. Cosmochim. Acta* 67, 681–691. doi: 10.1016/S0016-7037(02)01113-4

James, R. H., and Palmer, M. R. (2000). Marine geochemical cycles of the alkali elements and boron: the role of sediments. *Geochim. Cosmochim. Acta* 64, 3111–3122. doi: 10.1016/S0016-7037(00)00418-X

Jeffree, R. A., Markich, S. J., Lefebvre, F., Thellier, M., and Ripoll, C. (1995). Shell microlaminations of the freshwater bivalve *Hyridella depressa* as an archival monitor of manganese water concentration: experimental investigation by depth profiling using secondary ion mass spectrometry (SIMS). *Experientia* 51, 838–848. doi: 10.1007/BF01922440

Jochum, K. P., Weis, U., Stoll, B., Kuzmin, D., Yang, Q., Raczek, I., et al. (2011). Determination of reference values for NIST SRM 610-617 glasses following ISO guidelines. *Geostand. Geoanal. Res.* 35, 397–429. doi: 10.1111/j.1751-908X.2011.00120.x

Korte, C., Kozur, H. W., Bruckschen, P., and Veizer, J. (2003). Strontium isotope evolution of Late Permian and Triassic seawater. *Geochim. Cosmochim. Acta* 67, 47–62. doi: 10.1016/S0016-7037(02)01035-9

Labonne, M., and Hillaire–Marcel, C. (2000). Geochemical gradients within modern and fossil shells of *Concholepas concholepas* from northern Chile: an insight into U–Th systematics and diagenetic/authigenic isotopic imprints in mollusk shells. *Geochim. Cosmochim. Acta* 64, 1523–1534. doi: 10.1016/S0016-7037(99)00367-1

Lécuyer, C., Hutzler, A., Amiot, R., Daux, V., Grosheny, D., Otero, O., et al. (2012). Carbon and oxygen isotope fractionations between aragonite and calcite of shells from modern molluscs. *Chem. Geol.* 332, 92–101. doi: 10.1016/j.chemgeo.2012.08.034

Lorens, R. B., and Bender, M. L. (1980). The impact of solution chemistry on *Mytilus edulis* calcite and aragonite. *Geochim. Cosmochim. Acta* 44, 1265–1278. doi: 10.1016/0016-7037(80)90087-3

Lu, W., Oppo, D. W., Gebbie, G., and Thornalley, D. J. R. (2023). Surface climate signals transmitted rapidly to deep North Atlantic throughout last millennium. *Science* 382, 834–839. doi: 10.1126/science.adf1646

Luo, S., and Ku, T.-L. (1991). U-series isochron dating: A generalized method employing total-sample dissolution. *Geochim. Cosmochim. Acta* 55, 555–564. doi: 10.1016/0016-7037(91)90012-T

Marali, S., Schöne, B. R., Mertz-Kraus, R., Griffin, S. M., Wanamaker, A. D., Butler, P. G., et al. (2017). Reproducibility of trace element time-series (Na/Ca, Mg/Ca, Mn/Ca, Sr/Ca, and Ba/Ca) within and between specimens of the bivalve *Arctica islandica* – A LA-ICP-MS line scan study. *Palaeogeogr. Palaeoclimatol. Palaeoecol.* 484, 109–128. doi: 10.1016/j.palaeo.2016.11.024

Markich, S. J., Jeffree, R. A., and Burke, P. T. (2002). Freshwater bivalve shells as archival indicators of metal pollution from a copper–uranium mine in tropical northern Australia. *Environ. Sci. Technol.* 36, 821–832. doi: 10.1021/es011066c

Markulin, K., Peharda, M., Mertz-Kraus, R., Schöne, B. R., Uvanović, H., Kovač, Ž., et al. (2019). Trace and minor element records in aragonitic bivalve shells as environmental proxies. *Chem. Geol.* 507, 120–133. doi: 10.1016/j.chemgeo.2019.01.008

Marriott, C. S., Henderson, G. M., Belshaw, N. S., and Tudhope, A. W. (2004). Temperature dependence of δ7Li, δ44Ca and Li/Ca during growth of calcium carbonate. *Earth Planet. Sci. Lett.* 222, 615–624. doi: 10.1016/j.epsl.2004.02.031

Mashayek, A., Gula, J., Baker, L. E., Naveira Garabato, A. C., Cimoli, L., Riley, J. J., et al. (2024). On the role of seamounts in upwelling deep-ocean waters through turbulent mixing. *Proc. Natl. Acad. Sci.* 121, e2322163121. doi: 10.1073/pnas.2322163121

McCulloch, M. T., Winter, A., Sherman, C. E., and Trotter, J. A. (2024). 300 years of sclerosponge thermometry shows global warming has exceeded 1.5 C. *Nat. Climate Change* 14, 171–177. doi: 10.1038/s41558-023-01919-7

Meister, P., and Reyes, C. (2019). The carbon-isotope record of the sub-seafloor biosphere. *Geosciences* 9, 507. doi: 10.3390/geosciences9120507

Millward, G. E., Morris, A. W., and Tappin, A. D. (1998). Trace metals at two sites in the southern North Sea: results from a sediment resuspension study. *Continent. Shelf Res.* 18, 1381–1400. doi: 10.1016/S0278-4343(98)00049-1

Mukherjee, I., and Large, R. R. (2020). Co-evolution of trace elements and life in Precambrian oceans: The pyrite edition. *Geology* 48, 1018–1022. doi: 10.1130/G47890.1

Paton, C., Hellstrom, J., Paul, B., Woodhead, J., and Hergt, J. (2011). Iolite: Freeware for the visualisation and processing of mass spectrometric data. *J. Anal. Atom. Spectrom.* 26. doi: 10.1039/c1ja10172b

Philipp, E. E. R., and Abele, D. (2010). Masters of longevity: lessons from long-lived bivalves–a mini-review. *Gerontology* 56, 55–65. doi: 10.1159/000221004

Pohlman, J. W., Greinert, J., Ruppel, C., Silyakova, A., Vielstädte, L., Casso, M., et al. (2017). Enhanced CO_2 uptake at a shallow Arctic Ocean seep field overwhelms the positive warming potential of emitted methane. *Proc. Natl. Acad. Sci.* 114, 5355–5360. doi: 10.1073/pnas.1618926114

Poulain, C., Gillikin, D. P., Thébault, J., Munaron, J.-M., Bohn, M., Robert, R., et al. (2015). An evaluation of Mg/Ca, Sr/Ca, and Ba/Ca ratios as environmental proxies in aragonite bivalve shells. *Chem. Geol.* 396, 42–50. doi: 10.1016/j.chemgeo.2014.12.019

Price, G. D., and Pearce, N. J. G. (1997). Biomonitoring of pollution by *Cerastoderma edule* from the British Isles: a Laser Ablation ICP-MS study. *Mar. pollut. Bull.* 34, 1025–1031. doi: 10.1016/S0025-326X(97)00098-2

Raitzsch, M., Kuhnert, H., Hathorne, E. C., Groeneveld, J., and Bickert, T. (2011). U/Ca in benthic foraminifers: A proxy for the deep-sea carbonate saturation. *Geochem. Geophys. Geosys.* 12. doi: 10.1029/2010GC003344

Ren, J., He, G., Yang, Y., Yu, M., Deng, Y., Pang, Y., et al. (2024). Ultraselective enrichment of trace elements in seawater by Co-rich ferromanganese nodules. *Global Planet. Change* 239, 104498. doi: 10.1016/j.gloplacha.2024.104498

Rio, M., Roux, M., Renard, M., and Schein, E. (1992). Chemical and isotopic features of present day bivalve shells from hydrothermal vents or cold seeps. *PALAIOS*, 351–360. doi: 10.2307/3514821

Scholz, F., Hensen, C., De Lange, G. J., Haeckel, M., Liebetrau, V., Meixner, A., et al. (2010). Lithium isotope geochemistry of marine pore waters–insights from cold seep fluids. *Geochim. Cosmochim. Acta* 74, 3459–3475. doi: 10.1016/j.gca.2010.03.026

Scholz, D., Mangini, A., and Felis, T. (2004). U-series dating of diagenetically altered fossil reef corals. *Earth Planet. Sci. Lett.* 218, 163–178. doi: 10.1016/S0012-821X(03)00647-2

Schöne, B. R., Huang, X., Zettler, M. L., Zhao, L., Mertz-Kraus, R., Jochum, K. P., et al. (2021). Mn/Ca in shells of *Arctica islandica* (Baltic Sea)–A potential proxy for ocean hypoxia? *Estuarine Coast. Shelf Sci.* 251, 107257. doi: 10.1016/j.ecss.2021.107257

Schöne, B. R., Marali, S., Mertz-Kraus, R., Butler, P. G., Wanamaker, A. D., and Fröhlich, L. (2022). Importance of weighting high-resolution proxy data from bivalve shells to avoid bias caused by sample spot geometry and variability in seasonal growth rate. *Front. Earth Sci.* 10, 889115. doi: 10.3389/feart.2022.889115

Shangde, L., Wenyuan, S., Zhen, C., and Yipu, H. (1987). A new method for separation and determination of U and Th in deep-sea manganese nodules. *Acta oceanol. Sin.* 1), 87–93.

Takesue, R. K., Bacon, C. R., and Thompson, J. K. (2008). Influences of organic matter and calcification rate on trace elements in aragonitic estuarine bivalve shells. *Geochim. Cosmochim. Acta* 72, 5431–5445. doi: 10.1016/j.gca.2008.09.003

Thompson, W. G., Spiegelman, M. W., Goldstein, S. L., and Speed, R. C. (2003). An open-system model for U-series age determinations of fossil corals. *Earth Planet. Sci. Lett.* 210, 365–381. doi: 10.1016/S0012-821X(03)00121-3

Torres, M. E., Barry, J. P., Hubbard, D. A., and Suess, E. (2001). Reconstructing the history of fluid flow at cold seep sites from Ba/Ca ratios in vesicomyid clam shells. *Limnol. Oceanogr.* 46, 1701–1708. doi: 10.4319/lo.2001.46.7.1701

Torres, M. E., Bohrmann, G., Dubé, T. E., and Poole, F. G. (2003). Formation of modern and Paleozoic barite at continental margin methane seeps. *Geology* 31, 897–900. doi: 10.1130/G19652.1

Trofimuk, A. A., Cherskiy, N. V., and Tsarev, V. P. (1974). Mechanism of fractionation of isotopes of water and gas in crustal zones of hydrate formation. *Doklady Akademii Nauk SSSR* 215, 1226–1229.

Turekian, K. K., Cochran, J. K., Kharkar, D. P., Cerrato, R. M., Vaisnys, J. R., Sanders, H. L., et al. (1975). Slow growth rate of a deep-sea clam determined by 228Ra chronology. *Proc. Natl. Acad. Sci.* 72, 2829–2832. doi: 10.1073/pnas.72.7.2829

Vernon, R. H., and Clarke, G. L. (2008). Principles of metamorphic petrology. Cambridge University Press

Villemant, B., and Feuillet, N. (2003). Dating open systems by the 238U–234U–230Th method: application to Quaternary reef terraces. *Earth Planet. Sci. Lett.* 210, 105–118. doi: 10.1016/S0012-821X(03)00100-6

Wang, M., Chen, T., Feng, D., Zhang, X., Li, T., Robinson, L. F., et al. (2022). Uranium-thorium isotope systematics of cold-seep carbonate and their constraints on geological methane leakage activities. *Geochim. Cosmochim. Acta* 320, 105–121. doi: 10.1016/j.gca.2021.12.016

Wang, C., Guo, W., Li, Y., Dahlgren, R. A., Guo, X., Qu, L., et al. (2021). Temperature-regulated turnover of chromophoric dissolved organic matter in global dark marginal basins. *Geophys. Res. Lett.* 48, e2021GL094035. doi: 10.1029/2021GL094035

Wendt, K. A., Li, X., and Edwards, R. L. (2021). Uranium–thorium dating of speleothems. *Elements* 17, 87–92. doi: 10.2138/gselements.17.2.87

Xu, H., Du, M., Li, J., Zhang, H., Chen, W., Wei, J., et al. (2020). Spatial distribution of seepages and associated biological communities within Haima cold seep field, South China Sea. *J. Sea Res.* 165, 101957. doi: 10.1016/j.seares.2020.101957

Yao, H., Niemann, H., and Panieri, G. (2020). Multi-proxy approach to unravel methane emission history of an Arctic cold seep. *Quater. Sci. Rev.* 244, 106490. doi: 10.1016/j.quascirev.2020.106490

Zhao, L., Schöne, B. R., Mertz-Kraus, R., and Yang, F. (2017a). Insights from sodium into the impacts of elevated pCO_2 and temperature on bivalve shell formation. *J. Exp. Mar. Biol. Ecol.* 486, 148–154. doi: 10.1016/j.jembe.2016.10.009

Zhao, L., Schöne, B. R., Mertz-Kraus, R., and Yang, F. (2017b). Sodium provides unique insights into transgenerational effects of ocean acidification on bivalve shell formation. *Sci. Total Environ.* 577, 360–366. doi: 10.1016/j.scitotenv.2016.10.200